Search for shape isomers in ^{56}Ni

B. K. Dichter* and P. D. Parker
A. W. Wright Nuclear Structure Laboratory, Yale University, New Haven, Connecticut 06511

S. J. Sanders, R. R. Betts, and S. Saini†
Argonne National Laboratory, Argonne, Illinois 60439
(Received 12 December 1986)

An excitation function for the ^{40}Ca(^{16}O,^{28}Si*)^{28}Si* reaction has been measured between $74.925 \leq E_{lab} \leq 77.25$ MeV in 75-keV steps for $30° \leq \theta_{lab} \leq 60°$. Q-value and angular distributions were measured at each beam energy. Intermediate width ($\Gamma \simeq 200$ keV) structures are present in the excitation function at the 3—5% level of the cross section. An analysis of the present excitation function, together with one previously obtained for the inclusive elastic and inelastic ^{28}Si+^{28}Si scattering yields, indicates that the structures in the two excitation functions are correlated at an 80% confidence level. This suggests that the process responsible for the resonances is of compound-nuclear origin.

I. INTRODUCTION

Despite a quarter-century of extensive experimental and theoretical effort, a comprehensive model of heavy-ion resonance phenomena is still lacking. Explanations of heavy-ion resonances, first observed in the ^{12}C + ^{12}C system[1] and subsequently in systems as heavy as ^{28}Si + ^{28}Si,[2] can be generally classified in one of two seemingly distinct categories: (1) dynamical models[3–6] in which these resonances are viewed as being a consequence of both weak absorption and the existence of pockets in the interaction potential of the two ions, and (2) compound nucleus models,[7–10] in which shell stabilization of highly deformed compound nuclei may result in a set of states with unusually large overlap with heavy-ion decay channels. The current experimental data are insufficient to distinguish between these two alternatives and it is possible that both dynamical and structural features are present in the data. This paper reports on an attempt to test for a compound nucleus origin for the narrow resonance structures observed in the ^{28}Si + ^{28}Si system.

The ^{28}Si + ^{28}Si inclusive scattering yield with Q values between −22 and 0 MeV has been found[2] to be characterized by broad ($\Gamma = 2$—3 MeV) structures, each of which is further fragmented into narrower ($\Gamma \simeq 200$ keV) intermediate-width structures. The narrower structures appear in a correlated fashion in excitation functions for the various scattering states of the ^{28}Si + ^{28}Si system: elastic scattering, single 2^+ excitation, mutual 2^+2^+ and 2^+4^+ excitations, as well as excitations of higher lying excited states of the outgoing ^{28}Si nuclei. Detailed analysis of these data[11] has shown that the observed correlations do not arise from statistical fluctuations. The angular dependence of the large-angle elastic scattering cross section, measured at energies corresponding to the peaks of the broad structures, is well fitted by the squares of single Legendre polynomials,[12] with the order of the polynomials closely following the sequence of grazing angular momenta in the range of energies studied. At energies corresponding to minima between the broad structures, the angular distribution shapes are more complex and are not consistent with the angular dependence of squares of single Legendre polynomials.[12] These features suggest the interpretation of the intermediate-width structures as isolated resonances with spins near $40\hbar$. In the range of energies studied, the excitation energy of the compound nucleus is approximately 70 MeV and the level density[13] of $J = 40\hbar$ states at this excitation energy is of the order of 10^5 MeV^{-1}. The observed density of narrow resonances (3 MeV^{-1}) makes it unlikely that they correspond to normal, isolated, compound-nuclear states and, thus, a different mechanism must be used to account for these observations.

In light systems, notably ^{12}C + ^{12}C and ^{12}C + ^{16}O, entrance-channel models, such as the double-resonance model[3,4] and the band-crossing model[5] have been used to account for resonances observed in scattering processes. In such models the incident scattering state is explicitly coupled to other scattering states or reaction channels. The broad structures are generated by barrier top (virtual) resonances in the elastic channel. The fragmentation of the broad structures into the narrower structures is a result of the coupling of the virtual resonances to the much narrower (quasibound) resonances in the inelastic channels.

A double-resonance model calculation[14] by Thiel, Greiner, and Scheid reproduces some of the features of the ^{28}Si + ^{28}Si data. The authors explicitly couple the elastic ^{28}Si + ^{28}Si scattering channel to the single excitation of the first 2^+ state in ^{28}Si. The effects of other inelastic and reaction channels are taken into account by an imaginary potential. The calculations qualitatively reproduce the broad structures in the 80° and 90° excitation functions (measured with a 1 MeV step size) of elastic scattering and scattering to the first excited 2^+ state in ^{28}Si.[15] However, the intermediate-width structures evident in the 100-keV step size excitation function[2] are not reproduced. Furthermore the elastic scattering angular

distributions calculated using the potential of Thiel *et al.*[14,16] have large oscillations forward of $\theta_{c.m.}=60°$ which are not present in the data.[12] Another attempt to explain the $^{28}Si+^{28}Si$ data by means of an entrance-channel model was made recently by Khan and Beres,[17] using projection methods[18] within the framework of the doorway model.[19] The results of these calculations reproduce the low energy resolution 80° and 90° excitation functions.[12] However, no attempt was made to account for the high resolution data.

In a microscopic calculation of elastic $^{28}Si+^{28}Si$ scattering using the generator coordinate method, Langanke *et al.*[20] have shown that both virtual and quasibound resonances can exist in this system for partial waves up to $L=36\hbar$ for $E_{c.m.}\leq 60$ MeV. Working within the framework of the double-resonance mechanism,[4] the authors qualitatively reproduce the number and spacing of the intermediate-width structures that correspond to the $L=38\hbar$ broad structure of Ref. 2.

Another approach used to explain the $^{28}Si+^{28}Si$ data is based on the results of shell model calculations of energy surfaces of deformed rotating nuclei. The results of calculations for ^{24}Mg and ^{28}Si (Refs. 7 and 8) indicate the existence of potential energy minima at very large deformations. These minima have been identified with the virtual resonances of the entrance-channel models.[7] More recently, Bengtsson *et al.*[9] have studied potential energy surfaces of ^{56}Ni at high spin using the deformed harmonic oscillator, Nilsson, and Woods-Saxon cranked single particle potentials. The calculated shell corrections for $J=40\hbar$ indicate the existence of a potential energy minimum corresponding to a superdeformed, prolate nuclear shape with a 3:1 axis ratio. It has been suggested[21] that the intermediate-width structures in the elastic and inelastic scattering of $^{28}Si+^{28}Si$ result from the decay of states built upon the superdeformed minimum (shape isomers). The overlap of wave functions of the shape isomeric states with the much more numerous (10^5 MeV^{-1} in the spin and excitation energy range of interest), normal, more compact, compound-nuclear states might be small, thus inhibiting the mixing between the two types of states and enhancing the lifetimes of the isomers. The superdeformed states would be populated by all entrance channels that lead to ^{56}Ni formation, with a strength proportional to the decay width of the shape isomer into the entrance channel. The results of calculations of Bengtsson *et al.*[9] are very suggestive of such an interpretation, but leave a number of unresolved questions. For example, the experimentally measured energies of the $^{28}Si+^{28}Si$ resonances[12] lie approximately 15 MeV above the bottom of the calculated superdeformed minimum, while the calculated depth of the minimum is only about 5 MeV.

We have studied the $^{40}Ca(^{16}O,^{28}Si^*)^{28}Si^*$ reaction, reaching the same compound nucleus, ^{56}Ni, and covering the same excitation energy range of the compound nucleus ($E_{CN}\simeq 68$ MeV) as in the measurements of Betts *et al.*[2] for the $^{28}Si+^{28}Si$ system. The grazing angular momenta for the $^{16}O+^{40}Ca$ system in this energy range, calculated using the "quarter-point" recipe,[22] are approximately $1\hbar$ smaller than the measured angular momenta of the structures in $^{28}Si+^{28}Si$ scattering.[12] The observation of intermediate width structures in the $^{40}Ca(^{16}O,^{28}Si^*)^{28}Si^*$ reaction excitation function would be difficult to explain in an entrance channel picture which, at present, has no mechanism for large mass transfer. Further, the calculations of Langanke *et al.*[20] indicate that there are no quasibound resonances for $30\hbar\leq L\leq 40\hbar$ in the $^{16}O+^{40}Ca$ system.[20] Intermediate-width structures correlated with those observed by Betts *et al.*[2] would be strong evidence for a compound nucleus origin of the resonance states.

The experimental procedure and the normalization of the data are described in Sec. II. Section III contains the experimental results, discussion of the assumptions underlying the identification of the two-body, final-state yield in this experiment, statistical comparison of the data with those from the $^{28}Si+^{28}Si$ reaction, and an estimate of the decay width of the isomeric states into the elastic $^{16}O+^{40}Ca$ channel. The paper concludes with a summary of the results.

II. EXPERIMENTAL PROCEDURE

We have measured the $^{40}Ca(^{16}O,^{28}Si^*)^{28}Si^*$ reaction excitation function at beam energies $73.95\leq E_{beam}\leq 77.25$ MeV in 75 keV steps ($\Delta E_{c.m.}=54$ keV) and for angles $30°\leq\theta_{lab}\leq 60°$. The experiment was done using the MP Tandem Van de Graaf facility of the A. W. Wright Nuclear Structure Laboratory at Yale University. The target consisted of a 28 μg/cm^2 layer of 99.9% enriched ^{40}Ca evaporated onto a 10 μg/cm^2 carbon foil. As a consequence of the evaporation, a small amount (1.5 μg/cm^2) of ^{nat}Ta was also present on the target. Large angle scattering of ^{16}O from the ^{nat}Ta was used in the relative normalization of different runs, as will be described below. The target was placed with the ^{40}Ca layer facing toward the beam. The energy loss of the ^{16}O beam in traversing the target was approximately 90 keV. A liquid nitrogen cooled cold trap was placed around the target to help reduce carbon buildup.

The scattered ^{28}Si ions were detected using a gas-ionization counter[23] capable of measuring the energy deposited in the gas, E, the differential energy loss, ΔE, and the position of the ion along the length of the entrance aperture. Monitor detectors were located at 15°, 25°, and 112° with respect to the beam. The experimental arrangement as well as a schematic diagram of the ionization counter are shown in Fig. 1.

Particles entered the gas-ionization detector through a polypropylene window of approximately 80 μg/cm^2 areal density. The counter, which subtended the angular range of $30°\leq\theta_{lab}\leq 60°$, had an active depth of 20 cm and was filled with 30 torr of isobutane. This amount of gas was sufficient to fully stop the Si ions, although the most energetic ions with $Z<12$ were not stopped. A capacitively coupled cathode-grid assembly[24] was used to measure the total energy deposited in the gas by an incident ion. The energy threshold for detecting Si ions was 20 MeV and the measured energy resolution of the detector was 1.5%. The ΔE signal was obtained using a 1 cm wide anode strip near the front of the counter; the ΔE energy resolution

was better than 7%. The position of the incident particle was measured using a resistive wire and a charge division technique. The position resolution was approximately 1 mm, which corresponds to an angular resolution of 0.6°.

The absolute normalization was obtained using the measured yield from the $^{16}O + ^{40}Ca$ elastic scattering in the 15° detector and the known cross section for this process. The uncertainty in the absolute normalization, based on the known experimental uncertainties, is estimated to be 20%. A 600 mm^2 surface-barrier detector, with a 2.7 cm diam aperture, 10 cm away from the target and mounted at 112° with respect to the beam, was used to monitor the $^{16}O + ^{nat}Ta$ elastic scattering yield. This yield is insensitive to beam angle shifts and was, therefore, used to provide the relative energy-to-energy normalization. The ratio of elastically scattered ^{16}O in the 112° detector and in the gas-ionization detector was constant to within 1.5%, and this value was included in calculating the total experimental uncertainty.

During the running of the experiment, the radiation damage suffered by the polypropylene foil in the entrance window was severe enough to require the replacement of this foil approximately every 24 h of running time. The possibility that the foils were of different thickness necessitated the division of the data into five different sets of runs, each corresponding to a different entrance foil. A large number of overlap runs were made, so that the five such sets of runs could be normalized to each other; the normalization of only two sets of runs had to be adjusted, both by approximately 5%.

III. RESULTS AND DISCUSSION

A. Experimental results

The nuclear charge of the ions detected in the gas-ionization counter was identified using a standard E-ΔE algorithm. Once identified as a silicon, the ion was assumed to (1) be a ^{28}Si, and (2) come from the two body $^{16}O + ^{40}Ca \rightarrow ^{28}Si + ^{28}Si$ reaction. The justification of these assumptions will be discussed below. The two assumptions together with the measured values of E and θ_{lab} completely determine the reaction kinematics and make it possible, for example, to calculate the Q value of the reaction. The energy and angular resolution of the gas-ionization detector result in a Q-value resolution of 1.5 MeV full width at half maximum (FWHM). The 20 MeV energy threshold for detecting Si ions made the gas-ionization counter sensitive to events with $Q \geq -40$ MeV at the most forward angle and $Q \geq -20$ MeV at the most backward one. A typical Q-value spectrum, integrated over the angular acceptance of the detector, is shown in Fig. 2. The shape of the spectrum is well described by a Gaussian curve with a width parameter σ of 4 MeV, but

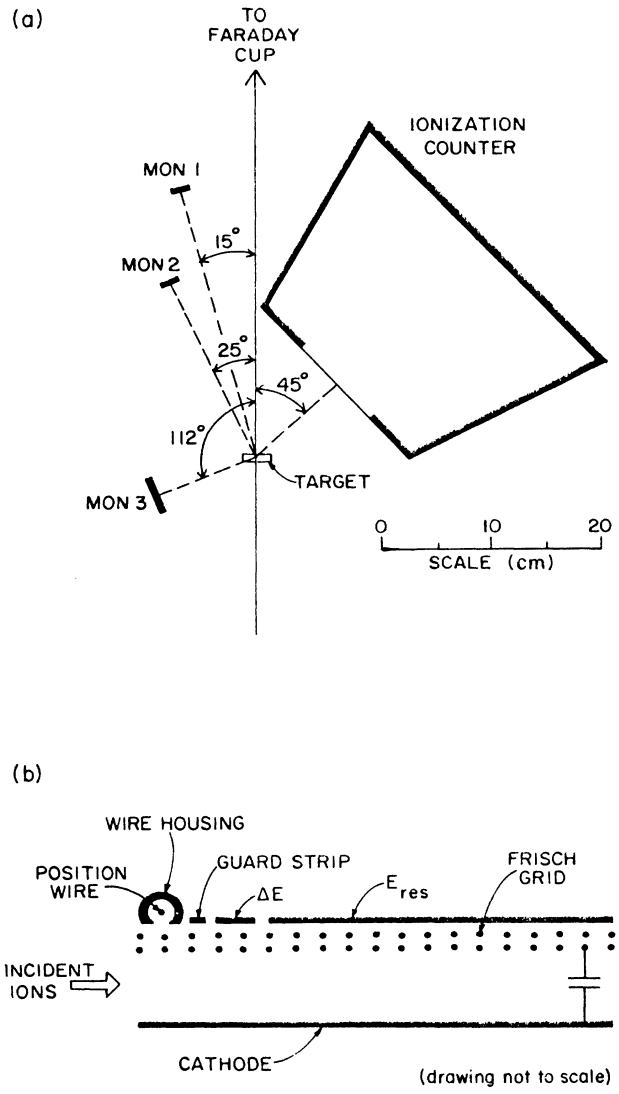

FIG. 1. (a) The diagram of the experimental setup. (b) Side cross sectional view of the gas-ionization detector.

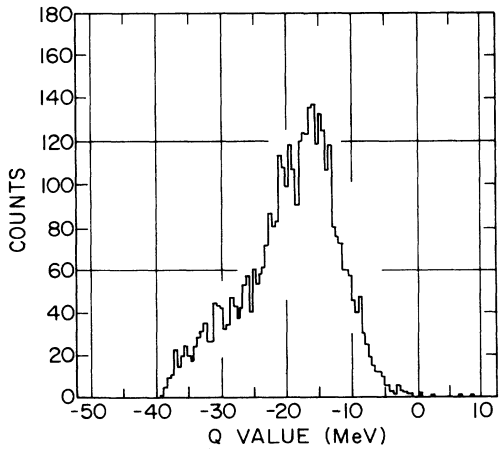

FIG. 2. Q-value spectrum for detected Si ions at $E_{lab} = 75$ MeV. The Q value is calculated assuming two-body kinematics (see text).

with a tail for events with $Q \leq -20$ MeV. In the subsequent analysis only the yield for events with $-20 \leq Q \leq 0$ MeV was used (see below).

The angular distributions of the Si ions were found to be consistent with a $d\sigma/d\Omega = 1/\sin(\theta_{\text{c.m.}})$ behavior (see Fig. 3). The total cross section was extracted from the measured differential cross sections using the assumption that this behavior continued to 0° and 180°. The total cross section thus obtained was divided by two to avoid the double counting inherent in the detection of experimentally indistinguishable fragments.

Some information regarding the time scale of this reaction can be extracted from the measured Q-value spectra and angular distributions. The mean Q value is independent of $\theta_{\text{c.m.}}$, in the range covered by this experiment, $50° \leq \theta_{\text{c.m.}} \leq 90°$, which indicates that the time scale is large compared with the time needed to fully damp out the center-of-mass kinetic energy. The angular distributions are consistent with a $1/\sin(\theta_{\text{c.m.}})$ behavior, which suggests that the ^{28}Si nuclei are produced in the decay of an intermediate state with a lifetime comparable to, or greater than, its rotational period. A more detailed discussion of these points can be found in Ref. 25.

The ^{40}Ca(^{16}O,^{28}Si*)^{28}Si* reaction excitation function for events with $-20 \leq Q \leq 0$ MeV is shown in Fig. 4. As can be seen, the cross section increases roughly linearly with increasing bombarding energy. Superimposed on this smooth behavior, at a 3—5% level of the cross section, are several structures with widths of the order of 200 keV. The degree of correlations between these structures and those found in the ^{28}Si(^{28}Si,^{28}Si*)^{28}Si* reaction excitation function will be discussed in Sec. III C.

B. Exit channel identification

As indicated above, the analysis of these data depends on two assumptions about the detected silicon ion: (1) it is a ^{28}Si, and (2) it is from the ^{28}Si + ^{28}Si exit channel of ^{16}O + ^{40}Ca scattering. The assumption that the detected Si ion is a ^{28}Si is supported by the fact that the experimentally measured mass distribution of the ^{16}O + ^{40}Ca reaction at 75 MeV is strongly peaked at mass $4N$ nuclei.[26] The evidence in support of the assumption that the detected Si ion, from events with $-20 \leq Q \leq 0$ MeV, comes from the ^{40}Ca(^{16}O,^{28}Si*)^{28}Si* reaction consists of two parts. One is a direct comparison with the results of another measurement of this reaction,[27] where the two fragments resulting from the ^{16}O + ^{40}Ca collision were detected in coincidence. The other is a result of the calculation (described below) of the ^{28}Si Q-value spectrum generated by the most likely contaminant process, ^{40}Ca(^{16}O,^{32}S*)^{24}Mg*, where the excited ^{32}S decays by α-particle emission and the daughter ^{28}Si is subsequently detected in the gas-ionization counter.

In a separate measurement of the ^{40}Ca(^{16}O,^{28}Si*)^{28}Si* reaction,[27] the outgoing fragments were detected in two position-sensitive, surface-barrier detectors. The measured energies and angles of the two ions, together with the assumption of a two-body final state, enable the reconstruction of the kinematics of the collision, including the masses of the fragments and the reaction Q value.[23] A comparison was made of the singles Si yield from the present experiment with the coincidence ^{28}Si + ^{28}Si yield from the preliminary study[23,27] in the angular range common to both experiments, $45° \leq \theta_{\text{lab}} \leq 60°$, at a beam energy

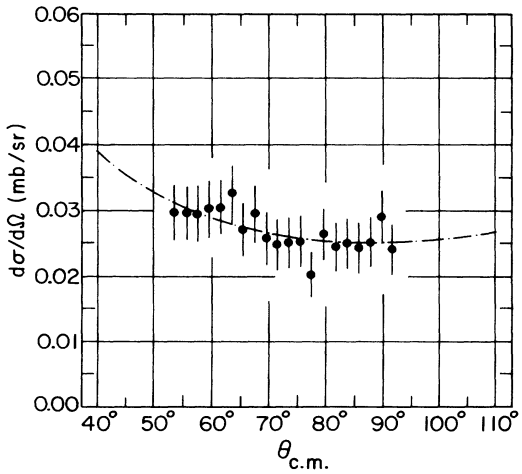

FIG. 3. The differential cross section for detected Si ions with $Q \geq -20$ MeV. The dotted-dashed line is a fit to the data assuming that $d\sigma/d\Omega \sim 1/\sin(\theta_{\text{c.m.}})$.

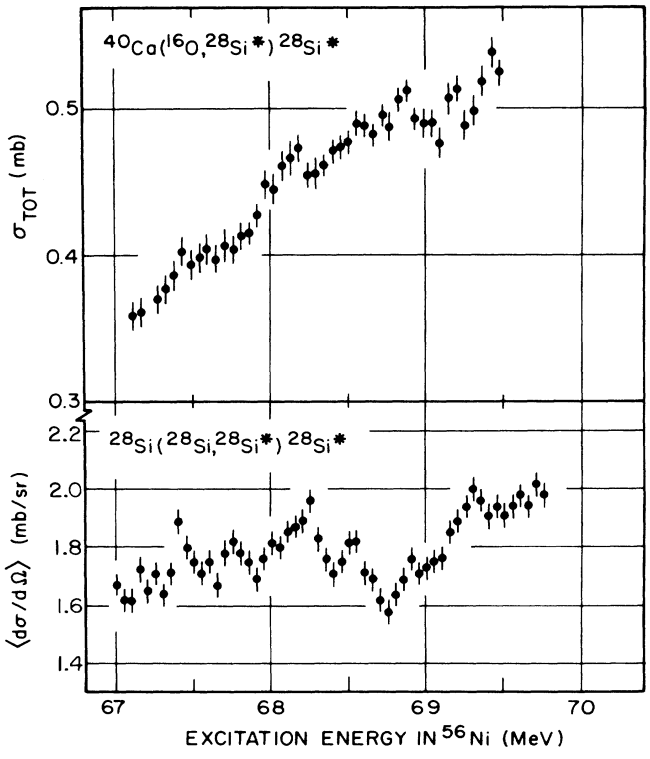

FIG. 4. Excitation functions of the ^{40}Ca(^{16}O,^{28}Si*)^{28}Si* and ^{28}Si(^{28}Si,^{28}Si*)^{28}Si* reactions are shown as a function of the excitation energy of the compound nucleus ^{56}Ni. The ^{28}Si(^{28}Si,^{28}Si*)^{28}Si* reaction data are taken from Ref. 2.

of 75.3 MeV. The yields of events with $Q \geq -20$ MeV from both experiments are the same to within the experimental uncertainty.[23] The coincidence experiment had a severe efficiency cutoff for events with $Q \leq -20$ MeV and, therefore, the yields of events with Q values more negative than -20 MeV could not be compared.

A Monte Carlo simulation of the ^{40}Ca(^{16}O,^{32}S*)^{24}Mg* reaction followed by the α-particle decay of ^{32}S was carried out in the following way (simplifying assumptions were made in this calculation because it is not the actual shape of the contaminant-event Q-value spectrum that is of interest, but only the most positive allowed values of that distribution). The ^{40}Ca(^{16}O,^{32}S*)^{24}Mg* reaction was assumed to have an angular and Q-value distribution similar to that measured in the ^{40}Ca(^{16}O,^{28}Si*)^{28}Si* reaction. The angular distribution was taken to be proportional to $1/\sin(\theta_{\text{c.m.}})$ and, for ease of computation, the Q-value distribution was chosen to be a Gaussian centered on $Q=-17$ MeV with a standard deviation of 5.5 MeV (the final results were found to be insensitive to changes in these values). The energy available for the excitation of the ^{32}S and ^{24}Mg, E^* can be written as $E^*=-(Q+Q_0)$, where Q_0 is the ground state reaction Q value. E^* was shared between the ^{32}S and ^{24}Mg in proportion to their masses, $E^*(^{32}\text{S})=(32/56)E^*$. If the excitation energy of the ^{32}S was above the s-wave α-particle emission threshold, an α-particle decay was assumed to take place with an angular distribution given by a constant $d\sigma/d\theta$. If the resulting daughter ^{28}Si was emitted into the angular region covered by the gas-ionization counter, the reaction Q value was calculated as if the ^{28}Si had come from the ^{28}Si + ^{28}Si exit channel.

The Q-value spectrum generated using this procedure contains no events with $Q \geq -25$ MeV. If the strict requirement that $E^*(^{32}\text{S})=(32/56)E^*$ is relaxed, that is for a given Q value $E^*(^{32}\text{S})$ is given by a Gaussian distribution with a mean of $(32/56)E^*$, contaminant events with apparent Q values less negative than -25 MeV become possible. However, even for values of the standard deviation of the individual fragment excitation energy distributions as large as 2.5 MeV, the contaminant event yield is confined to a region with apparent Q value more negative than -20 MeV. If angular momentum considerations of the α-particle decay and the angular momentum of the ^{32}S are included in the Monte Carlo calculation, this yield is shifted to even more negative Q values. The above considerations support the assumption that the singles $Z=14$ yield is very close to the ^{28}Si yield from the ^{40}Ca(^{16}O,^{28}Si*)^{28}Si* reaction for events with $Q \geq -20$ MeV, but may contain admixtures from a contaminant process for events with $Q \leq -20$ MeV.

C. Comparison with ^{28}Si + ^{28}Si data

A quantitative study of the correlations of the intermediate-width structures in the ^{40}Ca(^{16}O,^{28}Si*)^{28}Si* and ^{28}Si(^{28}Si,^{28}Si*)^{28}Si* reaction excitation functions was made using a statistical technique described by Saini and Betts.[11] Both excitation functions are plotted together for comparison in Fig. 4. New excitation functions (deviation functions), with the average behavior divided out, were constructed from the data.[11] The deviation functions, $D(E)$, are defined by

$$D_i(E)=\frac{Y_i-\langle\langle Y_i\rangle\rangle}{(\langle\langle Y_i^2\rangle\rangle-\langle\langle Y_i\rangle\rangle^2)^{1/2}}, \quad i=1,2$$

where $Y_i(E)$ is defined in terms of the measured excitation functions, $\sigma_i(E)$, and is given by

$$Y_i(E)=\frac{\sigma_i(E)}{\langle\sigma_i(E)\rangle},$$

where $\langle\ \rangle$ denotes an average over an energy interval large compared with the width of the intermediate width structures but small compared to the total energy range of the excitation function, and $\langle\langle\ \rangle\rangle$ denotes the average over the entire range of the excitation function. The $D_i(E)$ are, in turn, used to construct two new functions: the summed deviation function, $S(E)$, and the cross-correlation function, $C(E)$,

$$S(E)=\frac{1}{N}\sum_i D_i(E)=\tfrac{1}{2}[D_1(E)+D_2(E)],$$

$$C(E)=\frac{2}{N(N-1)}\sum_{i>j} D_i(E)D_j(E)=D_1(E)D_2(E),$$

The functions $S(E)$ and $C(E)$ and their probability distributions $P(S)$ and $P(C)$ can be compared to the values expected if the original data sets are uncorrelated.

The functions $S(E)$ and $C(E)$, extracted from the ^{16}O + ^{40}Ca and ^{28}Si + ^{28}Si data, are plotted together with correlation confidence limits in Fig. 5. The confidence limits were calculated using an analytical expression[28] for the $S(E)$ limits and by analysis of random spectra for the $C(E)$ limits. For two uncorrelated data sets with normally distributed $D(E)$, the $P(S)$ and $P(C)$ distributions have variances of 0.5 and 1.0, respectively. The variances of the distributions obtained from the data are 0.67 for $P(S)$ and 0.83 for $P(C)$, indicating, using the f test,[29] that the two data sets are correlated at an 80% confidence level. Finally, the mean of the experimentally derived $P(C)$ distribution, 0.31 ± 0.14, is two standard deviations from 0, the value for uncorrelated data sets.

D. Resonant widths

If the tentative evidence of correlations is accepted, then the ^{16}O + ^{40}Ca elastic decay widths of the ^{56}Ni resonances can be extracted from the data. A comparison of this width with the elastic ^{28}Si + ^{28}Si width, and both of these widths with the Wigner limits,[30] in the respective channels, is a first step in exploring the structure of the resonances underlying the intermediate-width structures. The reduced decay width γ^2 is given by

$$\gamma^2=\frac{\Gamma}{2P_L},$$

where P_L is the penetrability factor and Γ the observed width. The penetrability factor can be written in terms of the regular, F_L, and irregular, G_L, Coulomb wave functions, the wave number k, and the channel radius R,

$$P_L = \frac{kR}{F_L^2(kR)+G_L^2(kR)} ,$$

where $R = R_0(A_1^{1/3}+A_2^{1/3})$ and $R_0 = 1.5$ fm.

The observed widths in the entrance and exit channels, Γ_{in} and Γ_{out}, are related to the total resonance cross section, σ_{res}, by[31]

$$\sigma_{res} = (4\pi/k_{in}^2)(2L_{res}+1)\frac{\Gamma_{in}\Gamma_{out}}{\Gamma_{tot}^2} ,$$

where Γ_{tot}^2 is the total resonance width and L_{res} is the resonant angular momentum.

The total cross section, σ_{tot}, is assumed to consist of a resonant, σ_{res}, and a nonresonant, σ_{nr}, part with

$$\sigma_{tot} = \sigma_{res} + \sigma_{nr} .$$

An estimate of σ_{res} can be made from inspection of the excitation function. This division of σ_{tot} is motivated in the following way. The term in σ_{tot} resulting from interference between resonant and nonresonant processes in a reaction with a large number of possible final states is a sum of a large number of products of resonant and nonresonant amplitudes. If the phase angles of the resonant and nonresonant amplitudes in the various final states accessible to the system are uncorrelated, then this sum will, on the average, vanish.

This analysis was applied to the structure near $E_{CN} = 68.2$ MeV in the ^{40}Ca(^{16}O,^{28}Si*)^{28}Si* and ^{28}Si(^{28}Si,^{28}Si*)^{28}Si* reaction excitation functions. The ^{28}Si(^{28}Si,^{28}Si*)^{28}Si* reaction differential cross section[2] was converted to a total cross section. It was assumed that $d\sigma/d\Omega \sim 1/\sin(\theta_{c.m.})$ and a correction was made for the double counting inherent in that experiment. Inspection of the excitation functions gives $\sigma_{res} = 0.03$ mb for the ^{40}Ca(^{16}O,^{28}Si*)^{28}Si* reaction, $\sigma_{res} = 1.35$ mb for the ^{28}Si(^{28}Si,^{28}Si*)^{28}Si* reaction, and $\Gamma_{tot} = 200$ keV. The resonant angular momentum was assumed to be $L = 36\hbar$, which is in the range of angular momenta consistent in the ^{28}Si + ^{28}Si data at this energy.[12] The elastic ^{28}Si + ^{28}Si width is taken to be approximately 3 keV. This value was calculated from the elastic scattering data of Ref. 2 with the assumption that the magnitude of the $L = 36\hbar$ partial-wave term in the nonresonant amplitude is small, in the angular range of interest ($67° \leq \theta_{c.m.} \leq 95°$), compared to the corresponding term in the resonant amplitude and, therefore, the interference term in the differential cross section can be neglected. A 3 keV elastic ^{28}Si + ^{28}Si width is consistent with the magnitude of the $\theta_{c.m.} = 90°$ ^{28}Si + ^{28}Si elastic cross section quoted in Ref. 12, if it arises solely from the resonant amplitude.

The results of the analysis show that the ratio of the elastic resonance widths for the two reactions is of the order of 10 (see Table I). The value of γ^2_{O+Ca} calculated using this ratio is 8 eV, which is consistent with the measured 180° elastic ^{16}O + ^{40}Ca cross section,[32] if the enhanced backangle yield is assumed to come from the resonant process. Both of the elastic reduced widths greatly exceed their calculated statistical widths, which are a fraction of an eV.[13,33] Finally, both widths are less than 0.2% of the single particle Wigner limit, $\gamma^2_{s.p.}$, in their respective channels and the total ^{28}Si + ^{28}Si reduced (elastic and inelastic) exhausts less than 5% of the Wigner limit. This indicates that while the resonance wave function has a larger overlap with the wave function in the symmetric (^{28}Si + ^{28}Si) channel than with that in the asymmetric (^{16}O + ^{40}Ca) one, it is far from being a simple ^{28}Si + ^{28}Si molecular resonance.

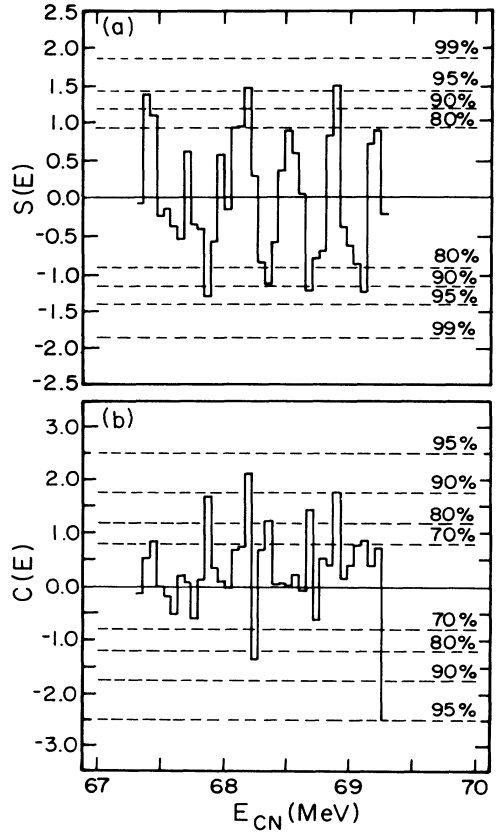

FIG. 5. The summed deviation function, $S(E)$, and the cross-correlation function, $C(E)$, for the excitation functions of the ^{40}Ca(^{16}O,^{28}Si*)^{28}Si* and ^{28}Si(^{28}Si,^{28}Si*)^{28}Si* reactions. The dashed lines are confidence levels (see text).

TABLE I. Listing of the relevant resonance width parameters for the structure at $E_{CN} = 68.2$ MeV.

Reaction	Γ_{tot} (keV)	Γ_{in} (keV)	γ^2_{in} (eV)	$\gamma^2_{in}/\gamma^2_{sp}$ (%)
O + Ca→Si + Si	200	0.1	8	0.01
Si + Si→Si + Si	200	3.1	108	0.2

IV. CONCLUSIONS

We have found intermediate width ($\Gamma \simeq 200$ keV) structures in the $^{40}Ca(^{16}O,^{28}Si^*)^{28}Si^*$ reaction excitation function, at a 3—5 % level of the cross section, at bombarding energies close to twice the Coulomb barrier energy. Comparison with the intermediate width structures found in elastic and inelastic $^{28}Si + ^{28}Si$ scattering[2] suggests that the structures are correlated, which would indicate that the underlying cause is a resonance process in the ^{56}Ni compound nucleus. The structure in the $^{40}Ca(^{16}O,^{28}Si^*)^{28}Si^*$ reaction excitation function cannot be reproduced by entrance-channel models, as currently formulated. The data are in qualitative agreement with deformed shell model calculations,[9] which predict superdeformed shape isomers of ^{56}Ni at high spin. These calculations, however, are far too schematic to enable any detailed comparisons with the data.

ACKNOWLEDGMENTS

We would like to than P. V. Magnus for his assistance in the data acquistion and Dr. B. B. Back for his comments on the manuscript. This work was supported by the U.S. Department of Energy under Contracts AC02-76ER03074 and W-31-109-ENG-38.

---

*Present address: Argonne National Laboratory, Argonne, IL 60439.

†Present address: Physics Department, University of Pennsylvania, Philadelphia, PA 19104.

[1]D. A. Bromley, J. A. Kuehner, and E. Almqvist, Phys. Rev. Lett. **4**, 365 (1960).

[2]R. R. Betts, B. B. Back, and B. G. Glagola, Phys. Rev. Lett. **47**, 23 (1981).

[3]H. J. Fink, W. Scheid, and W. Greiner, Nucl. Phys. **A188**, 259 (1972).

[4]W. Scheid, W. Greiner, and R. Lemmer, Phys. Rev. Lett. **25**, 176 (1976).

[5]Y. Abe in *Proceedings of the Second International Conference on Clustering Phenomena in Nuclei,* College Park, Maryland, 1975, edited by D. A. Goldberg, J. B. Marion, and S. J. Wallace (National Technical Information Service, Springfield, VA, 1975), p. 500.

[6]B. Imanishi, Nucl. Phys. **A125**, 33 (1969).

[7]H. Chandra and U. Mosel, Nucl. Phys. **A298**, 151 (1978).

[8]I. Ragnarsson, S. Åberg, and R. K. Sheline, Phys. Scr. **24**, 215 (1981).

[9]T. Bengtsson, M. Faber, M. Ploszajczak, I. Ragnarsson, and S. Åberg, Lund University Report 84/01.

[10]A. S. Umar and M. R. Strayer, Phys. Lett. **171B**, 353 (1986).

[11]S. Saini and R. R. Betts, Phys. Rev. C **29**, 1769 (1984).

[12]R. R. Betts, S. B. DiCenzo, and J. F. Peterson, Phys. Lett. **100B**, 17 (1981).

[13]W. Dilg, W. Schantl, H. Vonach, and M. Uhl, Nucl. Phys. **A217**, 269 (1973).

[14]A. Thiel, W. Greiner, and W. Scheid, Phys. Rev. C **29**, 864 (1984).

[15]R. R. Betts, S. B. DiCenzo, and J. F. Petersen, Phys. Rev. Lett. **43**, 253 (1979).

[16]A. Thiel, Ph.D. thesis, Institut für Theoretische Physik der Johann-Wolfgang-Goethe Universität, 1984.

[17]S. A. Khan and W. P. Beres, Phys. Rev. C **32**, 871 (1985).

[18]T. L. Larry and W. P. Beres, Phys. Rev. C **22**, 1145, (1980).

[19]H. Feshbach, A. K. Kerman, and R. H. Lemmer, Ann. Phys. (N.Y.) **41**, 230 (1967).

[20]K. Langanke, R. Stademann, and A. Weiguny, Phys. Lett. **112B**, 116 (1981).

[21]R. R. Betts, in *Proceedings of the 5th Adriatic International Conference on Nuclear Physics,* Hvar, Yugoslavia, 1984, edited by N. Cindro, W. Greiner, and R. Caplar (World-Scientific, Singapore, 1984), p. 33.

[22]J. S. Blair, Phys. Rev. **95**, 1218 (1954).

[23]B. K. Dichter, Ph.D. thesis, Yale University, 1985.

[24]D. Shapira, R. M. DeVries, F. W. Fulbright, J. Tóke, and M. R. Clover, Nucl. Instrum. Methods **118**, 116 (1975).

[25]S. J. Sanders, R. R. Betts, I. Ahmad, K. T. Lesko, S. Saini, B. D. Wilkins, F. Videbaek, and B. K. Dichter, Phys. Rev. C **34**, 1746 (1986).

[26]R. R. Betts, in *Proceedings of the Conference on Resonances in Heavy Ion Reactions,* Bad Honnef, 1981, Vol. 156 of *Lecture Notes in Physics* (Springer-Verlag, Berlin, 1982), p. 156.

[27]B. K. Dichter, S. J. Sanders, R. R. Betts, S. Saini, R. W. Zurmühle, and O. Hansen, Bull. Am. Phys. Soc. **28**, 1717 (1983).

[28]W. Mendenhall and R. L. Schaefer, *Mathematical Statistics with Applications* (Duxbury, North Scituate, Mass., 1973).

[29]*Handbook of Mathematical Functions,* edited by M. Abramowitz and I. Stegun (Dover, New York, 1972).

[30]T. Teichman and E. P. Wigner, Phys. Rev. **87**, 123 (1952).

[31]J. M. Blatt and V. F. Weisskopf, *Theoretical Nuclear Physics* (Springer-Verlag, Heidelberg, 1979).

[32]S. Kubono, P. D. Bond, and C. E. Thorn, Phys. Lett. **81B**, 140 (1979).

[33]J. Barrette, M. J. LeVine, P. Braun-Munzinger, G. M. Berkowitz, M. Gai, J. W. Harris, C. M. Jachcinski, and C. D. Uhlhorn, Phys. Rev. C **20**, 1759 (1979).